# One-to-six WDM multicasting of DPSK signals based on dual-pump four-wave mixing in a silicon waveguide

**Pu, Minhao; Hu, Hao; Ji, Hua; Galili, Michael; Oxenløwe, Leif Katsuo; Jeppesen, Palle; Hvam, Jørn Marcher; Yvind, Kresten**

*Published in:*
Optics Express

*Link to article, DOI:*
10.1364/OE.19.024448

*Publication date:*
2011

*Document Version*
Publisher's PDF, also known as Version of record

# One-to-six WDM multicasting of DPSK signals based on dual-pump four-wave mixing in a silicon waveguide

**Minhao Pu,* Hao Hu, Hua Ji, Michael Galili, Leif K. Oxenløwe, Palle Jeppesen, Jørn M. Hvam, and Kresten Yvind**

*DTU Fotonik, Department of Photonics Engineering, Technical University of Denmark, Build. 343, DK-2800 Kongens Lyngby, Denmark*
**mipu@fotonik.dtu.dk*

**Abstract:** We present WDM multicasting based on dual-pump four-wave mixing in a 3-mm long dispersion engineered silicon waveguide. One-to-six phase-preserving WDM multicasting of 10-Gb/s differential phase-shift-keying (DPSK) data is experimentally demonstrated with bit-error rate measurements. All the six multicast signals show error-free performance with power penalty less than 3.8 dB.



**OCIS codes:** (060.1155) All-optical networks; (060.4255) Networks, multicast; (190.4380) Nonlinear optics, four-wave mixing; (190.4390) Nonlinear optics, integrated optics; (130.7405) Wavelength conversion devices.

## References and links

1. X. Zhang, J. Wei, and C. Qiao, "Constrained multicast routing in WDM networks with sparse light splitting," J. Lightwave Technol. **18**(12), 1917–1927 (2000).
2. R. K. Pankaj, "Wavelength requirements for multicasting in all-optical networks," IEEE/ACM Trans. Netw. **7**(3), 414–424 (1999).
3. G. Contestabile, M. Presi, and E. Ciaramella, "Multiple wavelength conversion for WDM multicasting by FWM in an SOA," IEEE Photon. Technol. Lett. **16**(7), 1775–1777 (2004).
4. L. Xu, N. Chi, K. Yvind, L. Christiansen, L. K. Oxenløwe, J. Mørk, P. Jeppesen, and J. Hanberg, "7x 40 Gb/s base-rate RZ all-optical broadcasting utilizing an electroabsorption modulator," Opt. Express **12**(3), 416–420 (2004).
5. K. Inoue, T. Hasegawa, K. Oda, and H. Toba, "Multichannel frequency conversion experiment using fiber four-wave mixing," Electron. Lett. **29**(19), 1708–1709 (1993).
6. G. W. Lu, K. S. Abedin, and T. Miyazaki, "DPSK multicast using multiple-pump FWM in Bismuths highly nonlinear fiber with high multicast efficiency," Opt. Express **16**(26), 21964–21970 (2008).
7. C. S. Brès, A. O. J. Wiberg, B. P. P. Kuo, N. Alic, and S. Radic, "Wavelength Multicasting of 320-Gb/s Channel in Self-Seeded Parametric Amplifier," IEEE Photon. Technol. Lett. **21**(14), 1002–1004 (2009).
8. A. C. Turner-Foster, M. A. Foster, R. Salem, A. L. Gaeta, and M. Lipson, "Frequency conversion over two-thirds of an octave in silicon nanowaveguides," Opt. Express **18**(3), 1904–1908 (2010).
9. S. Zlatanovic, J. S. Park, S. Moro, J. M. C. Boggio, I. B. Divliansky, N. Alic, S. Mookherjea, and S. Radic, "Mid-infrared wavelength conversion in silicon waveguides using ultracompact telecom band derived pump source," Nat. Photonics **4**(8), 561–564 (2010).
10. M. A. Foster, A. C. Turner, R. Salem, M. Lipson, and A. L. Gaeta, "Broad-band continuous-wave parametric wavelength conversion in silicon nanowaveguides," Opt. Express **15**(20), 12949–12958 (2007).
11. M. Pu, H. Hu, M. Galili, H. Ji, C. Peucheret, L. K. Oxenløwe, K. Yvind, P. Jeppesen, and J. M. Hvam, "15 THz tunable wavelength conversion of picosecond pulses in silicon waveguide," IEEE Photon. Technol. Lett. **23**(19), 1409–1411 (2011).
12. R. Salem, M. A. Foster, A. C. Turner, D. F. Geraghty, M. Lipson, and A. L. Gaeta, "Signal regeneration using low-power four-wave mixing on silicon chip," Nat. Photonics **2**(1), 35–38 (2008).
13. M. A. Foster, A. C. Turner, J. E. Sharping, B. S. Schmidt, M. Lipson, and A. L. Gaeta, "Broad-band optical parametric gain on a silicon photonic chip," Nature **441**(7096), 960–963 (2006).
14. H. Rong, Y. H. Kuo, A. Liu, M. Paniccia, and O. Cohen, "High efficiency wavelength conversion of 10 Gb/s data in silicon waveguides," Opt. Express **14**(3), 1182–1188 (2006).
15. H. Hu, H. Ji, M. Galili, M. Pu, H. C. H. Mulvad, L. K. Oxenløwe, K. Yvind, J. M. Hvam, and P. Jeppesen, "Ultra-high-speed wavelength conversion in a silicon photonic chip," Opt. Express **19**(21), 19886–19894 (2011).
16. H. Ji, M. Pu, H. Hu, M. Galili, L. K. Oxenløwe, K. Yvind, J. M. Hvam, and P. Jeppesen, "Optical Waveform Sampling and Error-free Demultiplexing of 1.28 Tbit/s Serial Data in a Nano-engineered Silicon Waveguide," J. Lightwave Technol. **29**(4), 426–431 (2011).

#152131 - $15.00 USD Received 1 Aug 2011; revised 19 Sep 2011; accepted 7 Nov 2011; published 15 Nov 2011

17. A. Biberman, B. G. Lee, A. C. Turner-Foster, M. A. Foster, M. Lipson, A. L. Gaeta, and K. Bergman, "Wavelength multicasting in silicon photonic nanowires," Opt. Express **18**(17), 18047–18055 (2010).
18. S. Gao, E. K. Tien, Y. Huang, and S. He, "Experimental demonstration of bandwidth enhancement based on two-pump wavelength conversion in a silicon waveguide," Opt. Express **18**(26), 27885–27890 (2010).
19. S. Gao, E. K. Tien, Q. Song, Y. Huang, and O. Boyraz, "Ultra-broadband one-to-two wavelength conversion using low-phase-mismatching four-wave mixing in silicon waveguides," Opt. Express **18**(11), 11898–11903 (2010).
20. J. Hansryd, P. A. Andrekson, M. Westlund, Jie Li, and P.-O. Hedekvist, "Fiber-based optical parametric amplifiers and their applications," IEEE J. Sel. Top. Quantum Electron. **8**(3), 506–520 (2002).
21. M. Pu, L. Liu, H. Ou, K. Yvind, and J. M. Hvam, "Ultra-low-loss inverted taper coupler for silicon-on-insulator ridge waveguide," Opt. Commun. **283**(19), 3678–3682 (2010).
22. K. K. Lee, D. R. Lim, L. C. Kimerling, J. Shin, and F. Cerrina, "Fabrication of ultralow-loss Si/SiO(2) waveguides by roughness reduction," Opt. Lett. **26**(23), 1888–1890 (2001).
23. A. H. Gnauck and P. J. Winzer, "Optical phase-shift-keyed transmission," J. Lightwave Technol. **23**(1), 115–130 (2005).

## 1. Introduction

Multicasting is an important feature in a communication network, which can efficiently send a stream of information from a single source to multiple destinations [1, 2]. By using a multicasting technology, the amount of network resources can be significantly reduced compared to unicast-only networks. Optical layer multicasting could be implemented at fixed wavelengths by power splitting. An alternative is optical wavelength division multiplexing (WDM) multicasting, i.e., multicasting to different wavelengths. One of the most addressed techniques for WDM multicasting is all-optical multi-wavelength conversion (MWC), which replicates signals from one wavelength on multiple wavelengths. The WDM multicasting has been demonstrated in different devices including semiconductor optical amplifiers (SOAs) [3], electroabsorption modulators (EAMs) [4], and highly nonlinear fibers (HNLFs) [5–7], based on different nonlinear effects such as self-phase modulation (SPM), cross-phase modulation (XPM), cross-absorption modulation (XAM), and four-wave-mixing (FWM).

Recently, nonlinear effects in silicon waveguides have attracted considerable research interests due to compactness, large conversion bandwidth and complementary metal-oxide-semiconductor (CMOS) compatibility. Due to the strong light confinement in silicon waveguides with sub-micron dimensions, the group velocity dispersion (GVD), which is a critical parameter for parametric processes, can be engineered and thus one can achieve ultra-broadband wavelength conversion [8–11]. Previously, different nonlinear applications including signal regeneration [12], parametric amplification [13], wavelength conversion [14, 15], ultra-fast waveform sampling, and demultiplexing [16], have been demonstrated using silicon waveguides. Recently, silicon waveguides have also been used for a sixteen-way multicasting operation of 40-Gb/s none-return-to-zero (NRZ) data [17]. However, sixteen continuous wave (CW) tunable laser sources (TLSs) are needed to act as input signals and phase information is not preserved in the converted signals. All the above mentioned nonlinear applications are based on single-pump degenerate FWM. On the other hand, dual-pump FWM can be utilized to enhance the FWM conversion bandwidth [18] and a potential for multicasting operation based on dual-pump FWM in a silicon waveguide has also been demonstrated [19]. However, in that demonstration only one-to-two wavelength conversion was achieved, and without bit-error rate (BER) validation.

In this paper, we report one-to-six phase-preserving WDM multicasting of 10-Gb/s differential phase-shift-keying (DPSK) data based on dual-pump FWM in a dispersion engineered silicon waveguide. Error-free performances are achieved for all six multicast signals. Nine idlers are generated at the output of the silicon waveguide, which fully demonstrates dual-pump FWM. This is the first demonstration of WDM multicasting of a phase-modulated signal in a silicon waveguide.

## 2. Principle of operation

Figure 1 schematically illustrates the phase-preserving multicasting using dual-pump FWM. The frequencies of the two pump waves and the input DPSK signal wave are represented by $\omega_{p1}$, $\omega_{p2}$, and $\omega_s$, respectively. For a FWM process including three incident waves and all

#152131 - $15.00 USD Received 1 Aug 2011; revised 19 Sep 2011; accepted 7 Nov 2011; published 15 Nov 2011

possible degenerate and partially degenerate processes, nine new frequencies will be generated [20] as shown in Fig. 1.

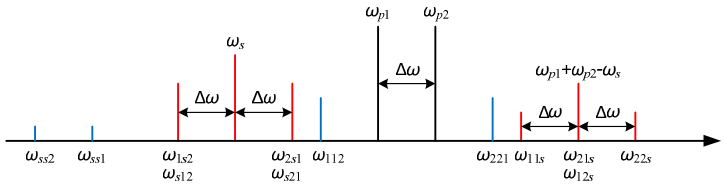


Fig. 1. Schematic illustration of one-to-six multicasting based on dual-pump four-wave mixing. Red components are the multicast channels and blue components are dummy channels.

Here, we denote each FWM generated wave as $\omega_{ijk}=\omega_i+\omega_j-\omega_k$, where the subscripts "*i*", "*j*" and "k" refer to three waves involved in the corresponding FWM process. The phase of the generated wave can be expressed as $(\Phi_i+\Phi_j-\Phi_k)$, where $\Phi_i$, $\Phi_j$ and $\Phi_k$ are the phases of the three waves involved in that process. To preserve the phase information of the original DPSK data (modulated with a $\pi$ phase shift) in a generated FWM wave, it requires that only one wave carries the original DPSK data ($\omega_s$) among the three wave ($\omega_i$, $\omega_j$, $\omega_k$) participating to that process. The generated nine idlers can be categorized into non-degenerate ($i\neq j$) and degenerate ($i=j$) FWM-converted idlers. All the non-degenerate FWM converted idlers at frequencies $\omega_s\pm(\omega_{p2}-\omega_{p1})$ and $\omega_{p1}+\omega_{p2}-\omega_s$ satisfy the aforementioned phase-preserving requirement and thus can copy all the information (both amplitude and phase) of the original DPSK data. However, the phase information is not preserved for the generated idlers at frequencies $\omega_{ss2}$ and $\omega_{ss1}$ since the original DPSK data signal wave ($\omega_s$) serves as the pump wave and acts twice in the corresponding FWM processes, resulting in doubled phase shifts and thus erases the phase information. Only two degenerate FWM idlers $\omega_{11s}$ and $\omega_{22s}$ carry the same phase information as the original DPSK data. For the generated idlers at frequencies $\omega_{112}$ and $\omega_{221}$, the original DPSK data signal wave ($\omega_s$) is not involved in the FWM processes. Therefore, there are six output signals (including the output signal at $\omega_s$) carrying the phase information of the input DPSK signal and a one-to-six WDM multicasting can be achieved. The frequency spacing between the six multicasting channels can be tuned to comply with the ITU grid by changing the frequency spacing between the three incident waves. As silicon waveguides offer ultra-broad conversion bandwidths [8, 11], the frequency spacing can be tuned over a large range covering the S-, C-, and L-bands. However, the frequency spacing still needs to be carefully chosen to avoid overlapping between the multicast and dummy channels which will cause distortions of the multicast signals. In addition, some multicast channel frequencies (e.g., $\omega_s\pm(\omega_{p2}-\omega_{p1})$ and $\omega_{p1}+\omega_{p2}-\omega_s$) are dependent on the two pump frequencies $\omega_{p1}$ and $\omega_{p2}$, therefore, these channel frequencies are correlated and will be tuned simultaneously if any one of the pump frequencies is tuned.

## 3. Experiment setup

The experimental setup for the one-to-six WDM multicasting of a 10-Gb/s DPSK signal in a silicon waveguide is shown in Fig. 2. Two pump waves are generated from two external cavity lasers ($ECL_1$ and $ECL_2$) at 1544.1 nm and 1548.1 nm, respectively. They are combined by a 3-dB coupler, amplified by an erbium-doped fiber amplifier (EDFA), and then filtered by a 5-nm optical band pass filter (OBPF). The signal wave, generated by another external cavity laser ($ECL_3$) at 1533.5 nm, is modulated by a Mach-Zehnder modulator into a 10-Gb/s DPSK signal, encoded by a pseudo-random bit sequence (PRBS) of $2^{31}$-1. The signal wave is amplified by an EDFA, filtered by a 1-nm OBPF, and then combined with the two pump waves through a 3-dB coupler. Two tapered fibers are used for coupling light into and out of the silicon waveguide. The polarization controllers (PCs) and polarizer are used to align the polarizations of the pump and signal waves to the TE polarization mode of the silicon waveguide.

#152131 - $15.00 USD Received 1 Aug 2011; revised 19 Sep 2011; accepted 7 Nov 2011; published 15 Nov 2011

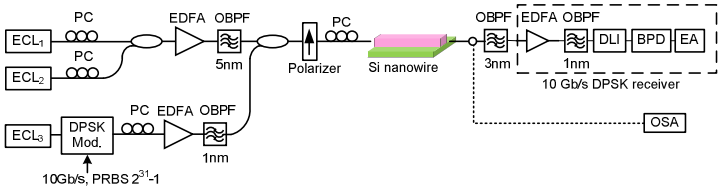


Fig. 2. Experimental setup for wavelength multicasting of 10-Gb/s DPSK data in a silicon waveguide.

The silicon waveguide is 3-mm long and its cross-sectional dimensions are 235 × 450 nm$^2$. It was fabricated on silicon-on-insulator (SOI) material using electron-beam lithography followed by reactive-ion etching. The silicon waveguide was inversely tapered at both ends and covered by a polymer waveguide for efficient coupling [21]. The propagation loss of the waveguide is ~4.3 dB/cm and the fiber-to-fiber coupling loss is ~5 dB. At the output of the silicon waveguide, each of the multicast signals is filtered out by a 3-nm Gaussian-shape tunable OBPF and detected by the 10-Gb/s DPSK receiver (shown by the dashed square in Fig. 2). In the receiver, the 10-Gb/s DPSK data signal is pre-amplified, filtered with a 1-nm rectangular-shape OBPF and then decoded by a one-symbol delay interferometer (DLI). The output of the DLI is detected by a balanced photodetector (BPD), followed by a 10-Gb/s error analyzer for BER measurement. An optical spectrum analyzer (OSA) is used to measure the output spectrum. Note that it is necessary to use a relatively broad (e.g., 3 nm) Gaussian-shape OBPF before the pre-amplification to ensure a sufficient input power to the EDFA since suppressing ASE noise from EDFA is essential to obtain a high OSNR for detection of the multicast signals.

## 4. Experiment results

Figure 3 shows the spectrum measured at the output of the silicon waveguide. The two CW pump waves and the input signal wave are denoted $\lambda_{p1}$, $\lambda_{p2}$, and $\lambda_s$, respectively. The input powers of the two pumps and the signal are 13.2 mW, 16.2 mW, and 9.5 mW, respectively. Due to the dual-pump FWM process, nine idlers ($I_1$-$I_9$) are generated as shown in Fig. 3.

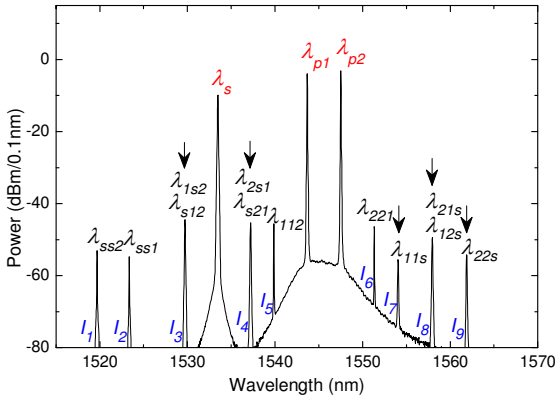


Fig. 3. Measured optical spectrum at the output of the silicon waveguide. The phase-preserving converted idlers are indicated by arrows.

As mentioned previously, not all the converted idlers carry the phase information of the original DPSK data. Only the three non-degenerate FWM idlers ($I_3$, $I_4$, and $I_8$) and two degenerate FWM idlers ($I_7$, and $I_9$), which are indicated by small arrows in Fig. 3, satisfy the previously mentioned phase-preserving requirement and thus can copy the phase information of the original DPSK data signal.

To characterize the performance of the WDM multicasting, we measured the BER of the 10-Gb/s back-to-back and the multicast 10-Gb/s DPSK data signals, as shown in Fig. 4. The

#152131 - $15.00 USD Received 1 Aug 2011; revised 19 Sep 2011; accepted 7 Nov 2011; published 15 Nov 2011

inset of Fig. 4 shows the eye-diagram of the input 10-Gb/s DPSK signal at 1533.5 nm. Error-free operations were obtained for all the multicast signals. It is also seen that there is no error floor for all the converted idler signals. Before the multicast signals were detected in the one-symbol DLI, we also measured the optical spectra of all the six multicast signals after the pre-amplification and filtering in the 10-Gb/s DPSK receiver as shown in Fig. 5. The insets of Fig. 5 show the corresponding eye diagrams of the output DPSK signals after demodulation. It is seen that all six converted idler signals have clear and open eyes, which also indicates the good quality of the multicast signal.

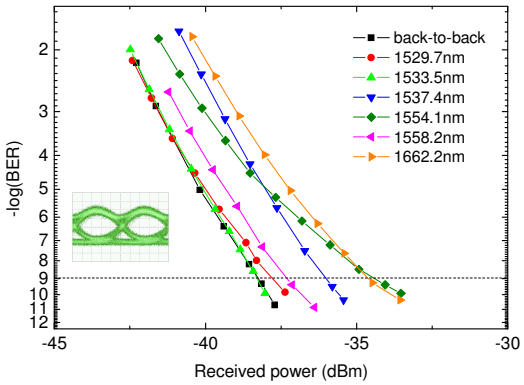


Fig. 4. BER measurement for the 10-Gb/s back-to-back DPSK signal, and the six multicast 10-Gb/s DPSK signals. Inset: eye-diagram of the input 10-Gb/s data signal at 1533.5 nm.

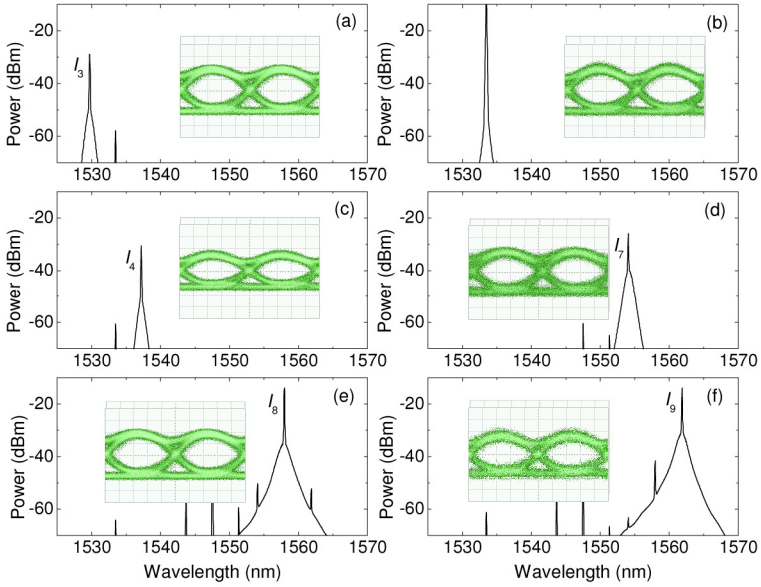


Fig. 5. Measured optical spectra of the amplified and filtered optical signals at different converted idler wavelengths. Insets: eye-diagrams of the wavelength-converted 10-Gb/s data signals at different wavelengths.

The performances of the multicast signals including optical signal-to-noise ratio (OSNR) measured in a resolution bandwidth of 0.1 nm at the output of the silicon waveguide, conversion efficiency, and power penalty at a BER of $10^{-9}$ are summarized in Table 1. It is obvious that the power penalty is very sensitive to the OSNR at the waveguide output. For the converted idlers $I_3$, $I_4$, and $I_8$ which have OSNRs larger than 20 dB, the power penalties are

#152131 - $15.00 USD Received 1 Aug 2011; revised 19 Sep 2011; accepted 7 Nov 2011; published 15 Nov 2011

less than 2.4 dB. On the other hand, the power penalties for converted idlers $I_7$ and $I_8$ are larger than 3.5 dB due to the relatively low OSNRs. The obtained OSNR is limited by the conversion efficiencies and the signal power. The conversion efficiency is highly dependent on the pump power, interaction length, and waveguide losses [15]. The relatively low conversion efficiencies are mainly due to the short waveguide and relatively high propagation loss. In addition, the power penalty also comes from the residual CW pumps and original signals that are not fully suppressed by the OBPF used to select the given multicast signal. The power penalty could be reduced by better filtering out the residual waves, increasing the pump power or reducing the propagation loss through optimization of the waveguide fabrication process [22]. In the present experiment the total pump power was ~16 dBm and launching higher power into the silicon waveguide could increase the conversion efficiency. However, silicon suffers from two-photon absorption (TPA) in the telecommunication wavelength range, thus the pump power should be kept below the TPA threshold (~39 dBm) [15] to suppress the free-carrier induced loss. For our current devices, the maximum launched power is limited further as high power could result in facet damage of the polymer waveguide. This can be avoided by increasing the cross-sectional area or replacing the used polymer by a more heat-resistant material (e.g., Benzocyclobutene (BCB)).

**Table 1. Performances of Six Multicast DPSK Signals**

| | Wavelength (nm) | OSNR (dB) | Conversion Efficiency (dB) | Power Penalty (dB) |
|---|---|---|---|---|
| $I_3$ | 1529.6 | 21.4 | –34.7 | 0.5 |
| $\lambda_s$ | 1533.5 | 52.5 | | 0.0 |
| $I_4$ | 1537.4 | 20.6 | –35.2 | 2.3 |
| $I_7$ | 1554.1 | 14.0 | –45.6 | 3.8 |
| $I_8$ | 1558.2 | 21.2 | –39.6 | 1.0 |
| $I_9$ | 1562.2 | 17.2 | –44.2 | 3.6 |

Compared with wavelength multicasting based on degenerate FWM [17], the dual-pump FWM offers a more efficient technique since it reduces the number of required laser sources, which simplifies the multicasting system and reduces the power consumption. In addition, the dual-pump FWM-based multicasting in this work is not only amplitude-preserving but also phase-preserving and thus is suitable for multicasting of DPSK or even more advanced modulation formats exploiting the phase dimension. Since the DPSK data format used in conjunction with balanced detection has 3-dB improved receiver sensitivity and a better tolerance to fiber nonlinearities compared to the conventional on-off keying (OOK) data format [23], the phase-preserving dual-pump FWM is a promising wavelength multicasting technique for future WDM optical networks. This technique is also suitable for higher bit rate multicasting, if the OSNRs of the multicast signals are enhanced by increasing the conversion efficiency of the silicon waveguides. To further increase the multicast channels, more pumps can be used to generate more FWM products [6].

## 5. Conclusion

We have experimentally demonstrated all-optical one-to-six WDM multicasting of 10-Gb/s DPSK data in a 3-mm long silicon waveguide. The multicasting operation is based on dual-pump FWM in silicon. The phase information of the input DPSK signal is successfully preserved and copied from one wavelength to six multicast wavelengths. In the BER measurements, all the six multicast signals show error-free performances with a maximum power penalty of 3.8 dB. The silicon waveguide could be useful for WDM multicasting applications in future WDM networks.

## Acknowledgment

This work was supported by the Danish Strategic Research Council and the EU FP7 via the projects NANO·COM and GOSPEL, respectively. The authors would like to thank associate Prof. Christophe Peucheret for helpful suggestions.

#152131 - $15.00 USD Received 1 Aug 2011; revised 19 Sep 2011; accepted 7 Nov 2011; published 15 Nov 2011